

**SYNTHESIS AND CHARACTERIZATION OF AUSTENITIC STAINLESS
STEEL BY MECHANICAL ALLOYING**

**A THESIS SUBMITTED IN PARTIAL FULLFILLMENT
OF THE REQUIREMENT FOR THE DEGREE OF**

Bachelor of Technology

in

Metallurgical and Materials Engineering

by

NIKUNJ AGARWAL (110MM0001)

ADARSH MOHANTY (110MM0365)



**DEPARTMENT OF METALLURGICAL AND MATERIALS
ENGINEERING**

NATIONAL INSTITUTE OF TECHNOLOGY, ROURKELA

May, 2014



National Institute of Technology, Rourkela

Certificate

This is to certify that the thesis entitled “**Synthesis and characterization of austenitic stainless steel by mechanical alloying**” being submitted by **Nikunj Agarwal (110MM0001)**, **Adarsh Mohanty (110MM0365)** for the partial fulfillment of the requirements of Bachelor of Technology degree in Metallurgical and Materials engineering is a bona fide thesis work done by them under my supervision during the academic year 2013-2014, in the Department of Metallurgical and Materials Engineering, National Institute of Technology Rourkela, India. The results presented in this thesis have not been submitted elsewhere for the award of any other degree or diploma.

Date:

(Prof. Swapan Kumar Karak)

Metallurgical and Materials Engineering

National Institute of Technology Rourkela

Acknowledgment

We would like to express our sincere gratitude to our guide Prof. Swapan Kumar Karak, Metallurgical and Materials Engineering, NIT Rourkela, for giving us the opportunity to work with him and providing excellent guidance and assistance throughout the project work. His constant criticism, advice, assertions, appreciation were very vital and irrevocable, giving us that boost without which it wouldn't have been possible for us to finish our project. We have received endless support and guidance from him, right from the development of ideas, deciding the experiments and methodology of work and this presentation. We wish to express our deep sense of gratitude to Dr.B.C.Ray, HOD, Metallurgical and Materials Engineering, NIT Rourkela for giving us an opportunity to work on this project. We would be highly obliged to extend our thanks to Mr. Uday Kumar Sahu and Mr Sandeep (M- Tech) for his immense support and help rendered while carrying out our experiments, without which the completion of this project would have been at stake. We would also like to thank all the staff members of MME Dept., NITR who helped us for this project.

Date:

Nikunj Agarwal (110MM0001)

Adarsh Mohanty (110MM0365)

Metallurgical and Materials Engineering

National Institute of Technology Rourkela

ABSTRACT

In the present study, an attempt on synthesis of austenitic stainless steel powder with nominal composition 70Fe-18Cr-8Ni (all in wt %) was milled by using planetary ball mill from 0 to 40 h. The 40 h milled powder was dispersed with 1.0 wt% nano-Y₂O₃ particles through blending and subsequently consolidated by conventional sintering at 1150°C for 1 h. The phase evolution and microstructure characterization at each stage of milling of 0h, 1h, 5h, 10h, 15h, 20h, 30h, 40h of the current alloys during milling were studied by using X-ray diffraction (XRD) and scanning electron microscope (SEM). The transformation of phase depends upon the milling time. With the increase of milling time, the intensity prominent peaks of XRD gradually decreases and peak broadening occurs. During the milling operation from 0h to 40h, the elements like Fe, Ni and Cr goes into the solid solution which increases the residual strain of the grains and decreases the crystal size of the particles. The crystallite size of austenitic stainless steel changes from 63.6µm to 5.49µm after 40 hours of milling. The sintering product, have been evaluated for determining different physical property (density and porosity) and mechanical property (hardness). It is found the hardness of alloy with dispersion of 1.0 wt% nano-Y₂O₃ particles was increased by 1.5 to 2 times higher than that of austenitic alloys.

Keywords: Synthesis, Mechanical alloying, Conventional Sintering, Characterization, X-ray diffraction (XRD) and scanning electron microscope (SEM)

Contents

Certificate	1
Acknowledgements	2
Abstract	3
Contents	4
List of figures	6

Chapter 1

Introduction

Introduction	8
--------------	---

Chapter 2

Literature Review

2.1	Stainless steel	8
2.2	Mechanical Alloying	10
2.3	Mechanism of mechanical alloying	17
2.4	Mechanical alloying of Austenitic Stainless Steel	20

Chapter 3

Experimental Details

3.1	Sample History	21
3.2	Synthesis by Mechanical Alloying	22
3.3	Compaction and Sintering	23
3.4	Characterization of mechanically alloyed powders and sintered pellets	23
3.4.1	X-ray diffraction analysis	23

3.4.2	Scanning electron microscope	24
3.5	Hardness measurement	25
3.6	Green Density/Sintered Density	26

Chapter 4

Results and Discussion

4.1	X-Ray Analysis	26
4.1.1	Phase evolution during mechanical alloying and sintering	26
4.2	SEM Analysis	29
4.2.1	Microstructural analysis of mechanical alloyed powders and sinter products	29
4.3	Density analysis	32
4.4	Hardness Study	33
4.5	Discussion	34

Chapter 5

Summary and Conclusion

5.0	Conclusion	34
-----	------------	----

References

36

List of Figures

Figure No.	Description	Page No.
Fig. 2.1	Kneading of powder as milling media collide	10
Fig. 2.2	Fritsch planetary mill	12
Fig. 2.3	The five stages of Mechanical alloying described by Benjamin and Volin mill.	16
Fig. 2.4	Schematic diagram depicting the ball motion inside the ball mill	18
Fig. 3.1	Philip's X-pert MPD X-ray diffractometer	24
Fig. 3.2	JEOL JSM-6480LV scanning electron microscope	25
Fig. 4.1	XRD patterns of mechanically alloyed powder at different milling times	27
Fig. 4.2	XRD Compositional Analysis of Base alloy (Alloy A)	28
Fig. 4.3	XRD Compositional Analysis of Y ₂ O ₃ dispersed alloy (Alloy B)	29
Fig. 4.4	SEM micrographs of the powder mixture milled for (a) 0h, (b) 1h, (c) 5h, (d) 10h, (e) 15h, (f) 20h, (g) 30h, and (h) 40h	31
Fig. 4.5	Hardness of sintered products (alloy A and alloy B)	33

List of Tables

Table No.	Description	Page No.
Table 1	Typical capacities of the different types of mills ^[4]	11
Table 2	Composition (initial) of the powder blends for mechanical alloying/milling	21
Table 3	Milling parameters	22
Table 4	Green density measurement of alloys before sintering	32
Table 5	Sintered Density Measurement	32
Table 6	Vickers hardness values of sintered products	33

1. INTRODUCTION

Austenitic Stainless steel is hard, strong and widely used alloy of chromium. The primary phase in these steel is austenite. Other physical properties of stainless steel are its high ductility, malleability, good conductor of heat and electricity, corrosion resistant. Stainless steel is capable of maintaining all these properties even at high temperatures which makes it suitable to be used in both high as well as low temperatures. Austenitic Stainless steel is used in various fields such as domestic, architectural /civil engineering, chemical/pharmaceutical (orthopedic application), oil and gas, medical etc. Dispersion of stainless steel with yttrium oxide further enhances its mechanical properties and strength. The oxide dispersed stainless steel is produced by the technique of powder metallurgy. This oxide dispersed stainless steel is used in many, high temperature process such as in automobile industries, nuclear reactors (fuel cladding) because of its excellent resistance to creep. Although chromium is the principal contributing factor to these extensive properties, nickel is a “powerful helpmate” .The process of, Mechanical alloying (solid state process) is a high energy ball milling process for producing composites with a controlled, even distribution of a second phase in a metallic matrix. Defects free alloys are produced by this process because of its high temperature.

The present work deals with the synthesis, characterization and mechanical properties of austenitic stainless steel by mechanical alloying. The aims of our work are

- ❖ Synthesis of 70.00Fe-19.00Cr-11.00Ni (alloy A), 70.00Fe-19.00Cr-11.00Ni with 1.0 wt% nano- Y_2O_3 dispersion particles (alloy B) through mechanical alloying.
- ❖ Mechanically alloyed powders at different stages of milling (0h, 1h, 5h, 10h, 15h, 20h, 30h, 40 h) as well as consolidated alloys were characterized using X-ray diffraction and Scanning Electron Microscopy.
- ❖ Hardness of the sintered samples was measured by using Vickers hardness tester.

We have divided the present thesis in 5 different chapters. In Chapter 1 and Chapter 2 a brief literature review is provided for austenitic stainless steel and mechanical alloying. Chapter 3 gives a brief detail of the experiments used, operating variables; data collected which is followed by discussions and the results of all the experiments in chapter 4. Chapter 5 provides with the summary of the present study followed by references after the end of the chapter.

2. LITERATURE SURVEY

2.1 STAINLESS STEEL

Stainless steel ^[1] contains around 10-30% chromium. Chromium is the basis for corrosion and oxidation resistance in stainless steel. One or more additional elements may be used in conjunction with chromium for most grades of stainless steels, but chromium is the key element contributing to corrosion resistance. When chromium is added to iron in relatively small amount (1 to 3 %), a modest increase in the corrosion resistance is evident. However, as the amount of chromium approaches approximately 10%, a dramatic increase in corrosion resistance takes place; such an alloy is virtually impervious to rusting from almost any outdoor exposure to normal atmospheres, such as rain, humidity, and temperature variations. This does not necessarily hold true in saline or industrial atmospheres.

Therefore, a minimum requirement for a stainless steel is that it contains at least 11% chromium and that is capable of resisting attack from normal atmospheric exposure. It is essential that both of these conditions are fulfilled for a steel to qualify as a stainless steel. Many highly alloyed iron-base alloys such as certain tool steel, contain more than 11% chromium, but because of their high carbon content, they do not meet the minimum requirements for stainless steel.

2.1.1 AUSTENITIC STAINLESS STEEL

The austenitic grades carry identification numbers of either 200 or 300, although most of them are 300 series alloys-the chromium nickel grades. The 200 series represents a more recent addition to the austenitic series in which some of the nickel is replaced by manganese. The austenitic grades are used most widely in corrosive environments, although some grades are used for elevated temperatures up to 700 degree centigrade.

Because the austenitic grades do not change their crystal structure on heating, they do not respond to conventional quench-hardening treatments. Therefore, the only heat treatment that are used for these grades are full annealing by rapid cooling from elevated temperatures and, in some instances, stress relieving. The 200 and 300 grades cannot be quench-hardened like alloy steels.

2.2 MECHANICAL ALLOYING

Mechanical alloying ^[2] is a high energy ball milling ^[3] process for producing composites with a controlled, even distribution of a second phase in a metallic matrix. It was first published in 1970's and introduced in the context of developing dispersion-strengthened alloys, in which strengthening by precipitations and dispersed oxides is combined. The process enables the development of special microstructures essential for achieving good high temperature mechanical properties in multi-phase powder metallurgy materials. In particular, the distribution of a second phase in a metallic, ductile matrix can be homogenized to a degree, which can be achieved otherwise only by chemical means. Also chemical reactions and formation of solid solutions can be obtained; in such cases the term 'reaction milling' is used. The often vexing problem of powder contamination has been analyzed and methods have been suggested to minimize it. The present understanding of the modeling of the MA process (shown in Fig. 2.1) is also under research.

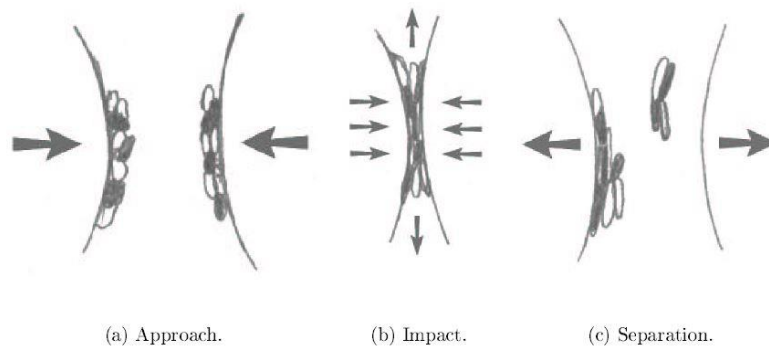


Fig. 2.1: Kneading of powder as milling media collide.

2.2.1 Attributes of Mechanical Alloying

- Production of fine dispersion of second phase particles (usually oxide)
- Extension of solid solubility limits
- Refinement of grain sizes down to nanometer range
- Synthesis of novel crystalline and quasi crystalline phases
- Development of amorphous (glassy) phases
- Disordering of ordered inter-metallic

- g. Possibility of alloying of difficult to alloy elements
- h. Inducement of chemical (displacement) reaction at low temperatures
- i. Scale-able process

2.2.2 Process Variables

MA is a complex process and a number of variables affect the desired product phase or microstructure. But all the process variables are not independent of each other all the time. For example, optimum milling time depends upon milling temperature. The following discussion is based on the assumption that other variables have no effect on the specific variable being discussed. Some of the most important parameters that have an effect on the final constitution of the powder are:

a. Types of mills

There are a number of different types of mill for carrying out MA (Fig 2.2). These mills are mainly differing in their speed of operation, capacity and their ability to control the operation by varying the temperature of milling. Thus, type of powder, the quantity of powder and the final constitution required decide the type of mill to be used.

Table 1: Typical capacities of the different types of mills ^[4]

Mill Type	Sample Weight
Mixer Mills	Up to 2x40g
Planetary mills	Up to 4x250g
Attritor	0.5-100kg
Uni –ball mills	Up to 4x2000g



Fig 2.2: Fritsch planetary mill

b. Milling container

It is also known as grinding vessel. During the process of grinding the grinding medium constantly strikes on the inner walls of the container and thus dislodges some material which may have joined the powder phase. This contaminates the powder and alters the chemistry of the powder. The shape of the container is also an important parameter, especially the internal design of the container. Both flat ended and round ended SPEX mill containers are being used these days. It has been found that alloying occurs at significantly higher rates in the flat-ended vials than in the round-ended containers^[5]. Some of the common materials used for the grinding

vessels are Hardened steel, tool steel, hardened Chromium steel, tempered steel, stainless steel, WC Co, WC-lined steel^[6] and bearing steel.

c. Milling speed

The Faster the mill rotates the higher would be the energy input into the powder. But, depending on the design of the mill there are certain limitations on the maximum speed that could be employed. For example, in a conventional ball mill increasing the speed of rotation will increase the speed with which the balls move. Above a critical speed, the balls will be pinned to the inner walls of the vial and do not fall down to exert any impact force. Therefore, the maximum speed should be just below this critical value so that the balls fall down from the maximum height to produce the maximum collision energy. Another limitation to the maximum speed is that at high speeds (or intensity of milling), the temperature of the vial may reach a high value. This may be advantageous in some cases where diffusion is required to promote homogenization and/or alloying in the powders. But, in some cases, this increase in temperature may be a disadvantage because the increased temperature accelerates the transformation process and results in the decomposition of supersaturated solid solutions or other metastable phases formed during milling^[6]. Additionally, the high temperatures generated may also contaminate the powders. It has been reported that during nano-crystal formation, the average crystal size increases and the internal strain decreases at higher milling intensities due to the enhanced dynamical recrystallization^[8]. The maximum temperature reached is different in different types of mills and the values vary widely.

d. Milling time

The time of milling^[7-8] is the most important parameter. Normally the time is so chosen as to achieve a steady state between the fracturing and cold welding of the powder particles. The times required vary depending on the type of mill used, the intensity of milling, the ball-to-powder ratio, and the temperature of milling. These times have to be decided for each combination of the above parameters and for the particular powder system. But, it should be realized that the level of contamination increases and some undesirable phases form if the powder is milled for times

longer than required ^[9]. Therefore, it is desirable that the powder is milled just for the required duration and not any longer.

e. Grinding medium

Some of the commonly used grinding medium are hardened chromium steel, tempered steel, stainless steel, WC Co and bearing steel. The density of the grinding medium should be high enough so that the balls create enough impact force on the powder. It is always desirable, whenever possible, to have the grinding vessel and the grinding medium made of the same material as the powder being milled to avoid cross contamination. The size of the grinding medium also has an influence on the milling efficiency. Generally speaking, a large size (and high density) of the grinding medium is useful since the larger weight of the balls will transfer more impact energy to the powder particles.

f. Ball to powder ratio

The ratio of the weight of the balls to the powder (BPR), sometimes referred to as charge ratio (CR), is an important variable in the milling process. This has been varied by different investigators from a value as low as 1:1^[10] to as high as 220:1. Generally speaking, a ratio of 10:1 is most commonly used while milling the powder in a small capacity mill such as a SPEX mill. But, when milling is conducted in a large capacity mill, like attrition, a higher BPR of up to 50:1 or even 100:1 is used. The BPR has a significant effect on the time required to achieve a particular phase in the powder being milled. The higher the BPR, the shorter is the time required. At a high BPR, because of an increase in the weight proportion of the balls, the number of collisions per unit time increases and consequently more energy is transferred to the powder particles and so alloying takes place faster. Several other investigators also have reported similar results. It is also possible that due to the higher energy, more heat is generated and this could also change the constitution of the powder. The amorphous phase formed may even crystallize if the temperature rise is substantial.

g. Extent of filling the vial

Since alloying among the powder particles occurs due to the impact forces exerted on them, it is necessary that there is enough space for the balls and the powder particles to move around freely in the milling container. Therefore, the extent of filling the vial with the powder and the balls is important. If the quantity of the balls and the powder is very small, then the production rate is very small. On the other hand, if the quantity is large, then there is not enough space for the balls to move around and so the energy of the impact is less. Thus, care has to be taken not to overfill the vial; generally about 50% of the vial space is left empty.

h. Milling atmosphere

The major effect of the milling atmosphere is on the contamination^[11] of the powder. Therefore, the powders are milled in containers that have been either evacuated or filled with an inert gas such as argon or helium. (Nitrogen has been found to react with metal powders and consequently it cannot be used to prevent contamination during milling, unless one is interested in producing nitrides.) High-purity argon^[12] is the most common ambient to prevent oxidation and/or contamination of the powder. It has also been noted that oxidation can be generally prevented or minimized in the presence of nitrogen ambient.

i. Process control agents

The powder particles get cold-welded to each other, especially if they are ductile, due to the heavy plastic deformation experienced by them during milling. But, true alloying among powder particles can occur only when a balance is maintained between cold welding and fracturing of particles. A process control agent (PCA) (also referred to as lubricant or surfactant) is added to the powder mixture during milling to reduce the effect of cold welding. The PCAs can be solids, liquids, or gases. They are mostly, but not necessarily, organic compounds, which act as surface-active agents. The PCA adsorbs on the surface of the powder particles and minimizes cold welding between powder particles and thereby inhibits agglomeration. The surface-active agents adsorbed on particle surfaces interfere with cold welding and lower the surface tension of the solid material. Since the energy required for the physical process of size reduction, E is given by the following equation (Eq. 1):

$$E = \gamma \cdot \Delta s \quad (1)$$

Where, ‘ γ ’ is the specific surface energy and ‘ Δs ’ is the increase of surface area, a reduction in surface energy results in the use of shorter milling times and/or generation of finer powders.

j. Temperature of milling

The temperature of milling is another important parameter in deciding the constitution of the milled powder. Since diffusion processes are involved in the formation of alloy phases irrespective of whether the final product phase is a solid solution, intermetallic, nanostructure, or an amorphous phase, it is expected that the temperature of milling ^[13] will have a significant effect in any alloy system. There have been only a few investigations reported where the temperature of milling has been intentionally varied. This was done by either dripping liquid nitrogen on the milling container to lower the temperature or electrically heating the milling vial to increase the temperature of milling. These investigations were undertaken to study the effect of milling temperature on the variation in solid solubility levels, or to determine whether an amorphous phase or a nano-crystalline structure forms at different temperature.

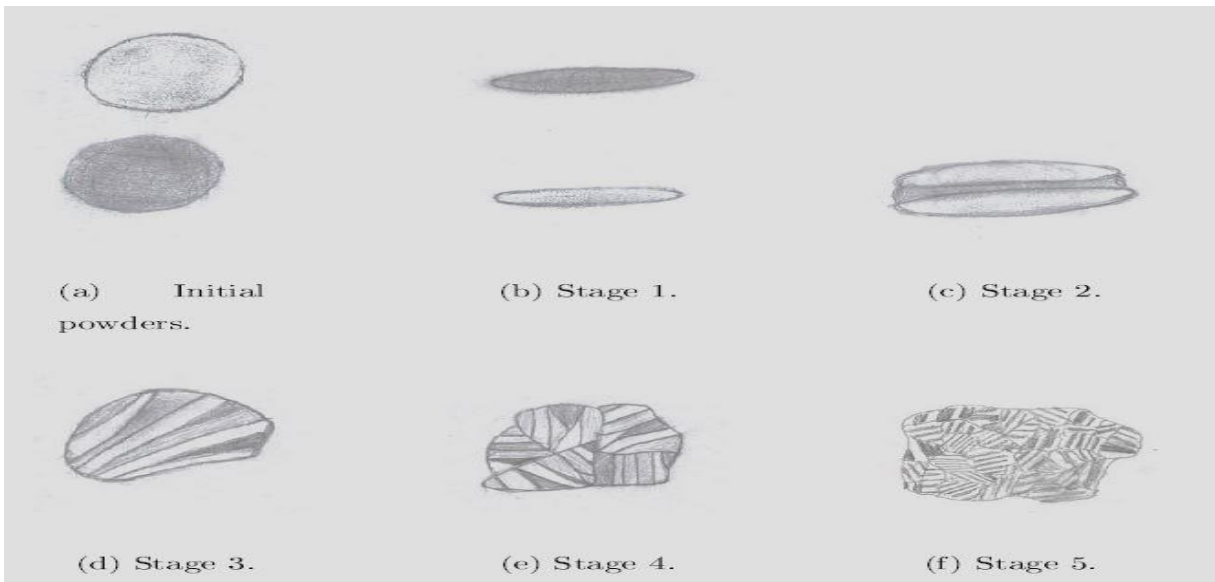


Fig. 2.3: The five stages of Mechanical alloying described by Benjamin and Volin.

2.3 MECHANISM OF MECHANICAL ALLOYING

The process consists of long period milling of mixtures, in which the main component (later the matrix) is generally ductile. As a result of the permanent high energy ball-powder interaction the ductile phase undergoes a continuous cycle of plastic deformation, fracture and re-welding processes, by which the fine dispersoids are implanted step-by-step into the interior of the ductile phase. This can be understood as a three stage process. In the first stage strong particle deformation ('mini-forging') and welding of particles are dominant, while the dispersoid is forced to cover the steadily increased surface of the ductile phase, which embrittles continuously. During the second stage the large lamellar-like particles formed are fractured, forming again new surfaces, which may pick up more of the dispersoid particles, re-weld and form finer lamellae (Fig.2.3). An equilibrium between deformation and welding on the one hand and fracturing on the other is reached (more or less) during the third stage, while homogenization proceeds, and the mechanical alloying process terminates. A considerable initial coarsening of the ductile phase can take place, when the starting particle size of the metal powder is very fine, while crystallite size decreases.

The efficiency of mechanical size-reduction processes is generally very low. Only about 0.1% of the spent energy in the conventional ball milling process is found in the generated new surfaces of the fine particles. The efficiency may be somewhat higher in high energy milling processes, but is still less than 1%. The percentage becomes larger when the energy necessary for crack propagation is considered. The sources of 'lost energy' are many: they include the elastic and plastic deformation of the particles, the kinetic energy of the particles in motion, impact and friction energy outside the powder, etc. The main cause of lost energy, however, is the generation of heat.

Fig. 2.4: shows a planetary ball mill. The difference from the conventional ball mill is the superposition of the single vessel rotation by rotation of the table supporting the fixed vessels, which accelerates the movement of the milling balls. Centrifugal accelerations up to 20 g (acceleration due to gravity) are possible.

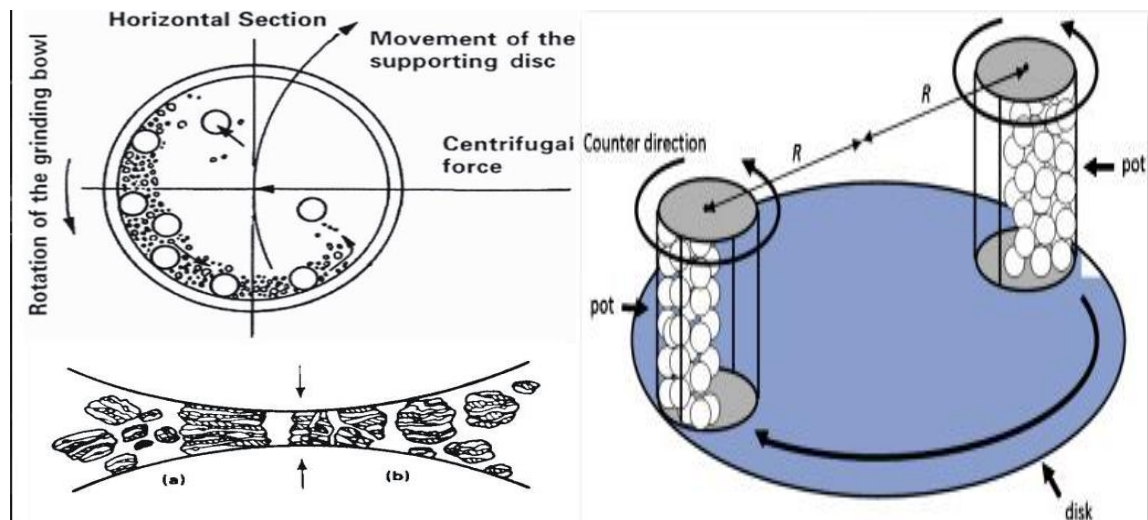


Fig. 2.4: Schematic diagram depicting the ball motion inside the ball mill.

In high-energy milling the powder particles are repeatedly flattened, cold welded, fractured and re-welded. Some amount of powder is trapped in between two steel balls whenever they collide. The powder particles are plastically deformed by the force of the impact leading to work hardening and fracture. The new surfaces created enabled the particles to weld together and this led to an increment in the particle size. In the early stages of milling, the particles were soft and their tendency to weld together and form large particles was high. A broad range of particle sizes developed, with some being as large as three times bigger than the starting particles. At this stage the composite particles had a characteristic layered structure which consisted of various combinations of starting constituents. With continued deformation, the particles get work hardened and fractured by a fatigue failure mechanism or by the fragmentation of fragile flakes. Fragments generated by this mechanism continued to reduce in size in the absence of strong agglomeration forces. At this stage, the tendency to fracture predominated over cold welding. The structure of the particles is steadily refined, due to continuous impact of grinding balls, but the particle size continued to be nearly the same. Consequently, the inter-layer spacing decreased and the number of layers in a particle increased. After milling for a certain length of time, steady-state equilibrium was attained when a balance was achieved between the rate of welding and the rate of fracturing, with an overall tendency to drive both very fine and large particles towards an intermediate size. At this stage each particle contained almost all of the starting ingredients and the particles reached saturation hardness due to the accumulated strain energy. The particle size distribution at this stage was narrow, because fragments smaller than average

grow through agglomeration of smaller particles at the same rate that particles larger than average were reduced in size.

Heavy deformation is introduced into the particles. This was manifested by the presence of variety of crystal defects such as dislocations, vacancies, stacking faults and increased number of grain boundaries. The presence of this defect structure enhanced the diffusivity of solute elements into matrix. Further, the refined microstructural features decreased the diffusion distances. Additionally, the slight increase in temperature during milling further aids the diffusion behavior and consequently, true alloying takes place amongst the constituent elements.

Enayati et al. 2007^[14] showed that when Fe–18Cr–8Ni and Fe–15Cr–15Ni elemental powder was alloyed mechanically, it led to the formation of a single-phase BCC solid solution of martensite with nano-scale sized grains of almost 15 nm. They observed that heat treatment of mechanical alloyed powder at 7000°C leads to formation of dual structured austenitic and martensitic phases. But the structure of Fe–15Cr–25Ni powder after milling remained as it was even after isothermal annealing resulted in the fully austenitic structure. Oleszak et al. 2006^[15] synthesized 316L austenitic steel powders in a planetary Fritsch P5 mill and found two-phased structures consisting of austenitic and martensitic stainless steel. Both the phases demonstrated nano-crystalline nature of crystallite size in the range 10–20 nm. After a very short period of milling, the martensite content reached 66%. As the milling time increased, the content of martensite decreased. This resulted in the formation of stable nano-crystalline austenitic stainless steel powder. Sintering was done by pulse current sintering technique to get dense hardened samples having austenitic nature. Sherif El-Eskandarany et al. 1994^[16] studied the synthesis of Fe-18Cr-8Ni elemental powder in rod mill at room temperature. After 1080ks of milling, they obtained homogeneous amorphous phase of austenitic stainless steel powder. They studied thermal behavior, structural morphology successfully. During first 2ks of milling, the elemental particles of Fe, Cr and Ni would not form any composition material. But as the milling time increased, they observed agglomeration of the particles started resulting in the increased particle size up to 50ks and became spherical and nano-crystalline after prolonged milling. Haghiri et al. 2009^[17] studied the phase transformation of ferritic to austenitic structure. They also studied the effect of argon and nitrogen gases on the structure of stainless steel using the elemental composition of Fe–18Cr–11Mn. They concluded their findings by showing argon gas atmosphere favors

formation of ferritic stainless steel powder and nitrogen gas atmosphere favors austenitic stainless steel powder after 120 h and 100 h respectively. They analyzed the variation of nitrogen content with milling time and they concluded that, the solubility of nitrogen increases with increase in milling time at N₂ atmosphere and it reaches as high as 0.65wt% after 100h.

2.4 MECHANICAL ALLOYING OF AUSTENITIC STAINLESS STEEL

Alloys with better mechanical properties have been developed by mechanical alloying and the success in their processing led to introduction of this method in dispersion strengthened austenitic stainless steel alloys. Presence of chromium oxide layer on the surface of the powder particles at the start of the milling always enhances improvement in the alloy properties. Austenitic stainless steel is a ductile material as we know and hence, cold welding occurs during milling which is minimized using an appropriate PCA^[18]. Stabilization of grain refinement occurs with the presence of oxide and carbide (formed during milling) type dispersions of finer size. Improvement in corrosion resistance, strength and fracture toughness is possible with the stabilization of grain refinement.

The production of powder containing a dispersion of reinforcements like TiO₂, Y₂O₃ in austenitic stainless steel matrix is only the first step in achieving the complete potential of dispersion hardened austenitic stainless steel alloys. The powders produced must be consolidated and then sintered or heat treated to develop coarse grains. So, as a thumb rule MA powder is always consolidated and heat treated to optimize grain structure and properties. But, the consolidation should be done in such a way that it doesn't lead to any inhomogeneity in the matrix. During sintering grain growth is inevitable but it should be in an optimum amount only. This is because despite of improving creep resistance it may lead to a less ductility and strength.

3. EXPERIMENTAL DETAILS

This chapter begins with a brief description of sample history. Two different alloy compositions were synthesized by Mechanical Alloying and have been used for the present study. After the description of sample history; mechanical alloying, compaction and sintering, equipment and techniques utilized for characterization of the two alloy systems have been systematically narrated.

3.1 SAMPLE HISTORY

The alloys were synthesized from austenitic stainless steel powders (SS 304-L) through mechanical alloying route. Base alloy system includes Iron (>99.5% pure), Chromium (>99.5% pure) and Nickel (>99.5% pure) powders. Further Y_2O_3 powder was added as reinforcement by blending machine. For base alloy preparation ball mill vial was filled with austenitic stainless steel powders. And for Y_2O_3 dispersed alloy 1 weight percentage of Y_2O_3 powder was added. During the milling process toluene was added as a process controlling agent. It helps in protecting the milled powders from oxidation. Toluene gets adsorbed on the surface of the powder particles and minimizes cold welding between powder particles and thereby also inhibits agglomeration. Another advantage is that the milled powder easily achieved amorphization by using wet milling media as toluene.

After 40 hour of ball milling two different alloy compositions were synthesized, i.e., one as the base alloy and another by blending of base alloy with Y_2O_3 reinforcement which are summarized in table 3.1.

Table 2: Composition (initial) of the powder blends for mechanical alloying /milling

Alloy	Y_2O_3 (wt. % of Alloy A)	Ni (wt. %)	Cr (wt. %)	Fe (wt. %)
A	0.0	11.0	19.0	70.00
B	1.0	11.0	19.0	70.00

3.2 SYNTHESIS BY MECHANICAL ALLOYING

Mechanical alloying of SS 304-L alloy (Fe-70%, Cr-19%, and Ni-11% namely Alloy A) and 1.0 wt% Y_2O_3 dispersed SS 304-L alloy was carried out using a planetary ball mill with hardened chrome steel container and balls. The diameter of hardened steel balls was 8mm and volume of the jar was 500 ml. During the synthesis of alloy using planetary ball mill, the ball to powder weight ratio was 10:1. As mentioned earlier, toluene was added to avoid agglomeration of powders during milling, prevent undue oxidation and ensure sufficient yield after the completion of milling. The milling was performed at 300 rpm speed of the planetary mill for up to 40h and at intervals of 0, 1, 5, 10, 15, 20, 30 and 40 hours the powder samples were collected to characterize the effect of milling time on the powder particles. The as milled powders were characterized by means of X-ray diffraction, using a standard diffractometer (*PhilipsXPERT MPD*) with Ni-filtered Cu K_α radiation ($\lambda = 0.154051$ nm). The compositional and morphological study was done by using a JEOL/EO type SEM/EDS.

Table 3: Milling parameters

Parameter	Value
Milling speed	300rpm
Balls/powder ratio	10:1
Ball diameter	8 mm
PCA	Toluene
Weight of powder	25g
Grinding medium	Cr steel
Milling time	40 h(pause mode every 30 min)
Type of mill	Planetary mill

3.3 COMPACTION AND SINTERING

The milled powder was then mixed with Y_2O_3 in a definite proportion (1wt %) by blending for 3 hours in a blending machine. The mixtures were taken for compaction using cold pressing machine. The mixtures were compacted under 6 tons of pressure to attain green strength for the samples. This forms round disk specimens of 9.8mm diameter and height 4.8mm for alloy A & 6.7mm for alloy B

The pellets obtained after compression were sintered in a furnace at 1150°C for 1 hour. To generate an inert atmosphere Argon gas at a pressure of 10^{-6} tor was blown inside the furnace to protect the pellets against oxidation and any other unnecessary chemical reactions.

3.4 CHARACTERIZATION OF MECHANICALLY ALLOYED POWDERS

The mechanically alloyed powders were analyzed by X-Ray Diffraction, SEM to understand the topographical characteristics and get information about elements and phases present in the powder after different hours of milling as mentioned earlier. XRD and SEM of sintered samples were also carried out in order to understand the effect of temperature and compression on the elements and phases present in the alloy synthesized.

3.4.1 X-RAY DIFFRACTION ANALYSIS

X-ray diffraction (XRD) studies were carried out for the purpose of identity and phase evolution at different stages of milling and also after sintering by using the Ni-filtered Cu-K α radiation (having wavelength of 0.154051 nm) in a Phillip's X'pert PRO high resolution X-ray diffractometer (Fig. 3.1). The X-ray source was operated at a voltage of 40 kV and current of 35 mA. The diffraction angle was varied in the range of 20-100 degrees while the scanning rate was 0.05degree/s. The XRD data diffraction patterns were analyzed with the help of Phillip's X'pert software. Compositional analysis of the alloy powders was also carried out with the help of XRD which confirmed the presence of Y_2O_3 in the reinforced alloy powder.



Fig. 3.1: Philips X-pert MPD X-ray diffractometer

3.4.2 SCANNING ELECTRON MICROSCOPY

Microstructure characterization, morphology and particle size determination was carried by a JEOL JSM-6480 LV scanning electron microscope (Fig. 3.2). Both the secondary electron (SE) mode and back scattered electron mode (BSE) were used as per the requirement.



Fig. 3.2: JEOL JSM-6480LV scanning electron microscope.

3.5 HARDNESS MEASUREMENT

To reveal the mechanical properties of the synthesized material micro-hardness measurement was carried out in a micro-hardness tester. Hardness studies of compact sintered samples were carried out by using Vickers micro hardness tester. For that sample preparation was done primarily by using 1/0, 2/0, 3/0 and 4/0 emery papers there after cloth polishing was done. Hardness was measured on all the samples using Wolpert Vickers hardness tester. Loads of 100g for dwell time of 10 seconds and a square base diamond pyramid indenter with an included angle of 360° between the faces were used during hardness measurement. As a result of the indenter's shape, the impression on the surface of the specimen was a square. The length of the diagonals of the square was measured through a microscope fitted with an ocular micrometer. Machine itself displays the hardness value in Vickers Pyramid Number (HV) or Diamond Pyramid Hardness (DPH). A minimum of 3 readings were taken on each sample and checked for consistency.

3.6 GREEN DENSITY / SINTERED DENSITY

The density of the pellet after compaction is called green density which is much greater than the density of the starting powders though green density is not uniform. Therefore the properties vary over the volume and also depend on the pressure in compaction. The density of the compact after sintering is called sintered density. The sintering density is measured by using Archimedes principle.

4. RESULTS AND DISCUSSION

4.1 X-RAY ANALYSIS

4.1.1 Phase evolution during mechanical alloying and sintering

Fig. 4.1 shows the XRD patterns of the as milled alloy powder with increasing milling times. Initially, the XRD peaks were more prominent and sharp, later on the peaks started broadening. After 30h and 40h of milling, it was observed that broadening of peak of only FCC-solid solution (Fe, Cr, Ni) was present. It was apparent that the milled product in each case was a single-phase face centered cubic (FCC) solid solution indicating that Cr and Ni completely dissolve in Fe during high-energy ball milling for 30-40 hours. The broadening of peak was associated with the accumulated lattice strain as well as reduction in crystal size. Moreover, the shifting of peak to the right side with an increase in milling time indicated that the 40 h milling time was more prominent to get fast amorphization. By the increase in strain and fast amorphization, the mechanical properties of the alloy can be developed further.

The first and the most interesting observation was that the Fe peaks tend to broaden as milling time increases. According to the Scherrer's formula we know that as crystallite size decreases peak tends to broaden. So it can be inferred that the Fe crystallite size decreases as milling time increases.

Secondly, the Cr and Ni peaks, which were clearly visible after 2h of milling, disappeared after about 30h of milling. The disappearance of Cr and Ni peaks reveals that Cr and Ni is getting diffused inside the Al lattice to form a solid solution which is the fundamental step of alloying.

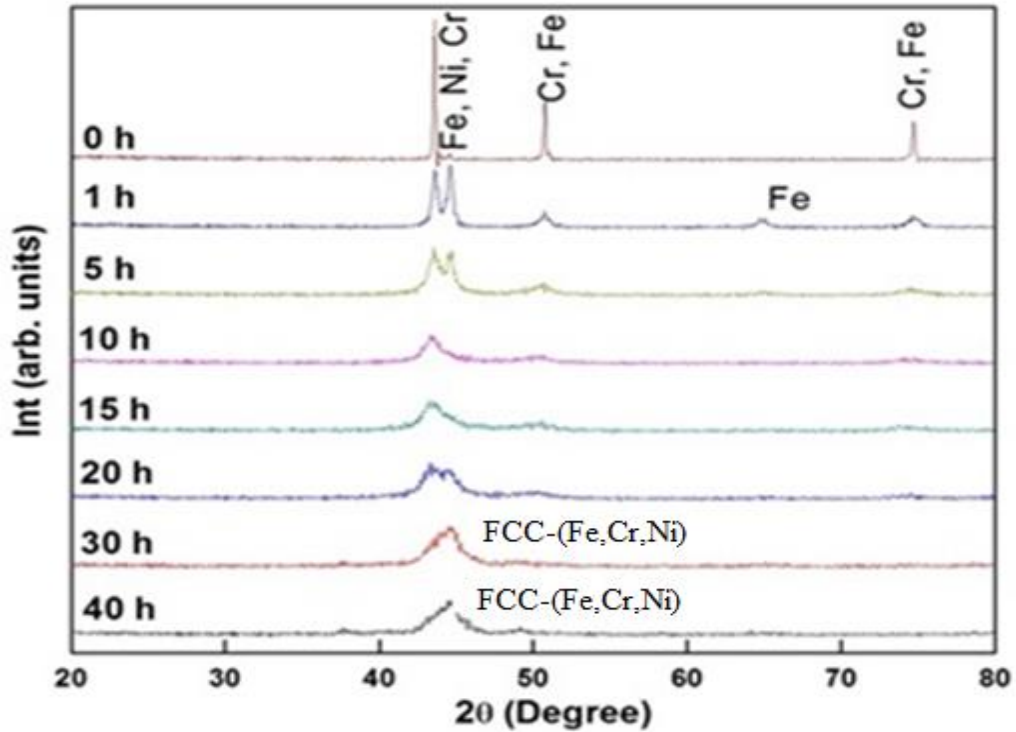


Fig. 4.1: XRD patterns of mechanically alloyed powder at different milling times

4.1.2 Compositional analysis of mechanical alloyed powders by XRD

Fig. 4.2 shows the elemental analysis of the base alloy after 40 hour of milling, which was carried out to investigate the chemical composition of the base alloy powder. The XRD confirms the presence of Fe, Cr and Ni and some minor impurities such as oxygen.

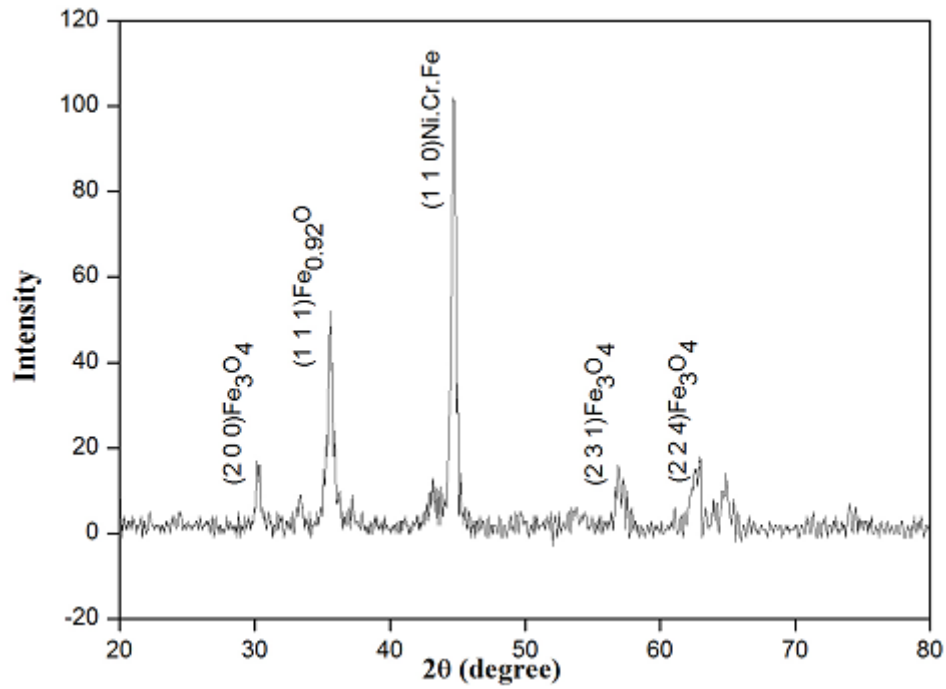


Fig. 4.2: XRD Compositional Analysis of Base alloy (Alloy A)

The XRD analysis results of base alloy with 1wt% Y_2O_3 powders is shown in Fig. 4.3 which confirms the presence of Yttrium.

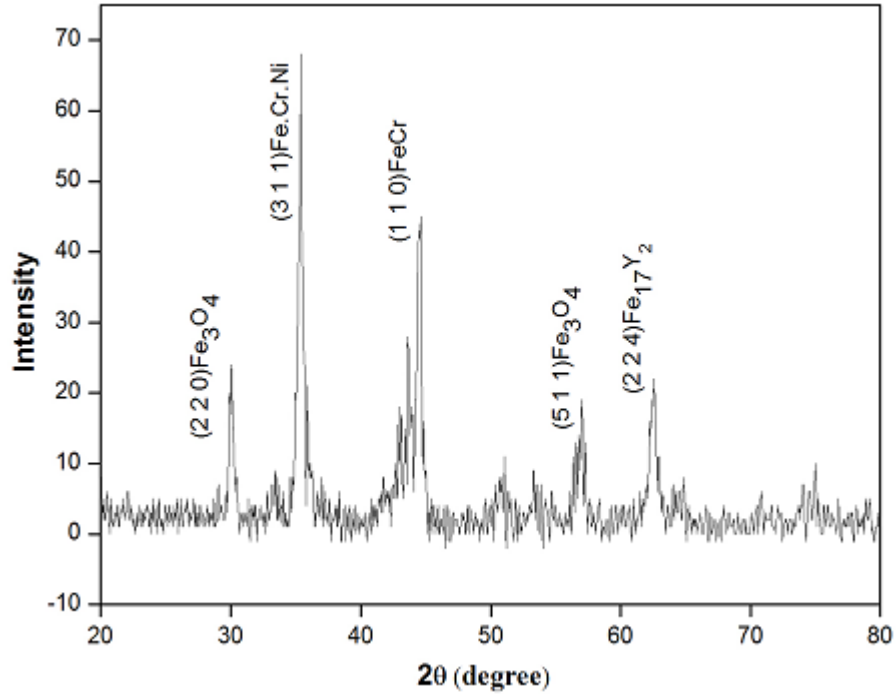


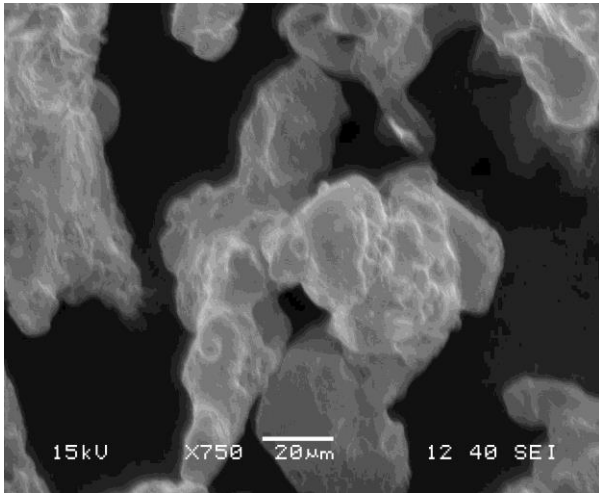
Fig 4.3: XRD Compositional Analysis of Y_2O_3 dispersed alloy (Alloy B)

4.2 SEM ANALYSIS

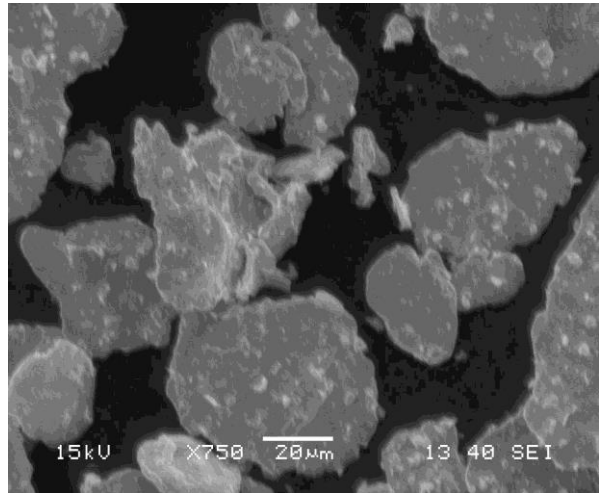
4.2.1 Microstructural analysis of mechanical alloyed powders and sinter products

Figs. 4.4 (a-g) show scanning electron microscopy of the austenitic stainless steel alloy during each stage of milling (0h, 5h, 10h, 15h, 20h, 30h, and 40h, respectively). At 0h of milling, the apparent particle size was observed to have a value of $63.66\mu\text{m}$, after 1 h of milling the average particle size was reduced to $56.1\mu\text{m}$. Further milling up to 5 h, 10h, 15h, 20h, 30h and 40h resulted in an average particle size of $28.6\mu\text{m}$, $22.0\mu\text{m}$, $12.2\mu\text{m}$, $8.29\mu\text{m}$, $7.75\mu\text{m}$ and $5.49\mu\text{m}$ respectively.

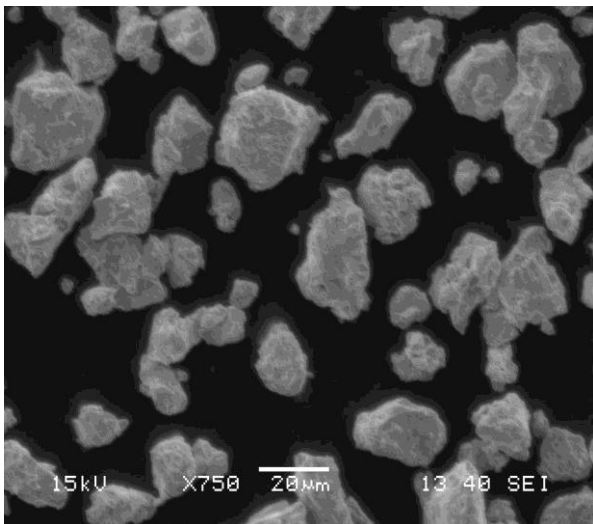
As we know that during mechanical alloying continuous cold welding, fracturing and re-welding of particles take place. This fact is well illustrated in the following micrographs. After 20 hours of milling coarser Chromium and Nickel particles have welded and as the milling was continued further these laminar shaped particles have transformed to equiaxed grains.



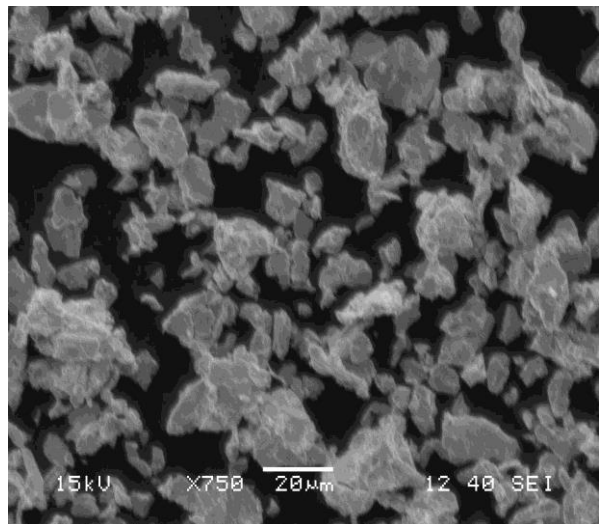
(a). 0 h



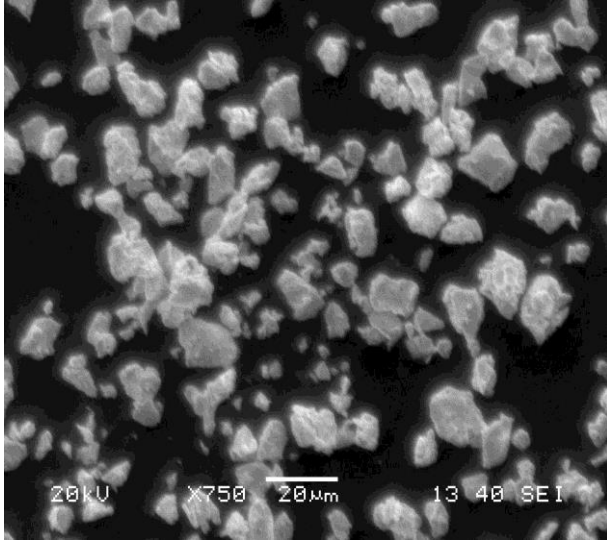
(b). 1 h



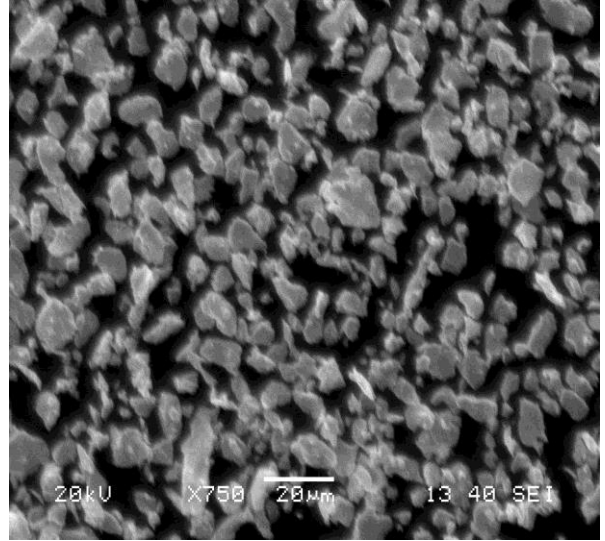
(c). 5 h



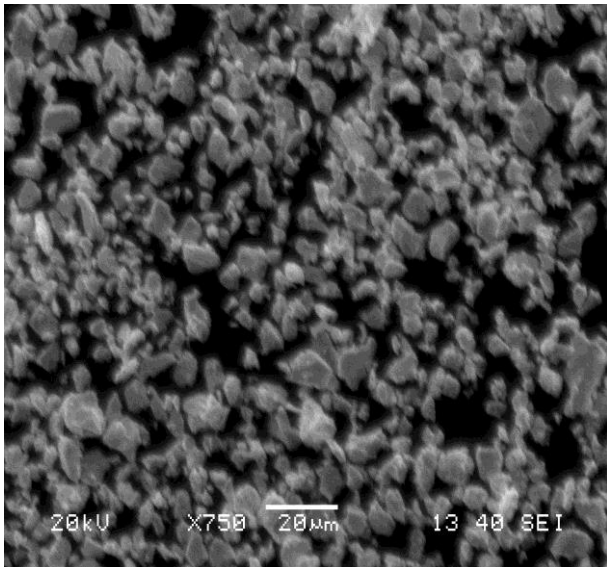
(d) 10 h



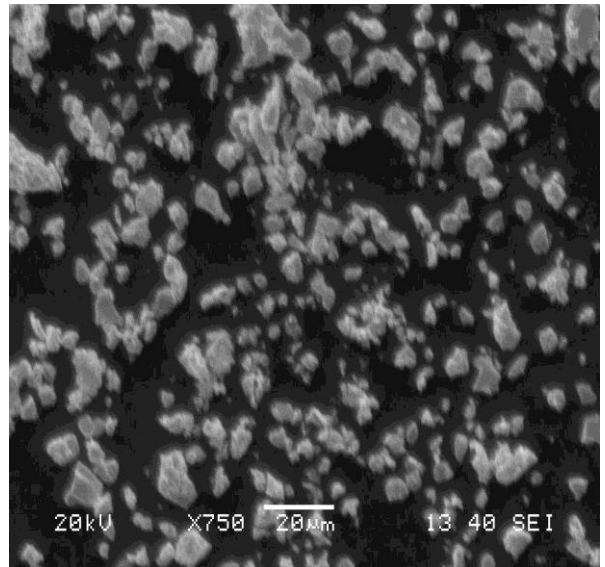
(e). 15 h



(f). 20 h



(g). 30 h



(h). 40 h

Fig.4.4: SEM micrographs of the powder mixture milled for (a) 0h, (b) 1h, (c) 5h, (d) 10h, (e) 15h, (f) 20h, (g) 30h, and (h) 40h.

4.3 Density analysis

4.3.1 Density Measurement before Sintering

Green Density is measured before sintering by the usual formula of mass upon volume. After compaction the disks have same diameter but different heights (in Table 4), where the mass is calculated after sintering. It is observed that the green density increases substantially after the addition of 1 wt% Y_2O_3 .

Table 4: Green density measurement of alloys before sintering

Alloy System	Mass(g)	Height(mm)	Diameter(mm)	Green Density(g/cc)
Alloy A	1.650	4.8	9.8	4.55
Alloy B	2.371	6.7	9.8	4.69

4.3.2 Density measurement after sintering:

The density measured after sintering is the sintered density. The sintering was done at 1150°C by the means of conventional sintering. It is a bit more uniform measurement of density than the green density. It is measured by using Archimedes formula (shown in Table 5).

Table 5: Sintered Density Measurement

Alloy System	Sintered Density (g/cm ³)	Porosity (%)
Alloy A	7.92	8.0
Alloy B	7.97	3.0

4.4 HARDNESS STUDY

The hardness values of the sintered alloys in both alloy A and alloy B (1.0 wt. % Y_2O_3) are summarized at Table 6. It is found (Fig.4.5) that the hardness of alloy B (1.0 wt. % Y_2O_3) is 1.5 to 2 times higher than that of alloy A.

Table 6: Vickers hardness values of sintered products

Alloy Systems	Average Hardness (HV)
Alloy A	206.35
Alloy B	367.94

The hardness increases with addition of Y_2O_3 reinforcement. It is observed that the hardness of the Y_2O_3 dispersed alloy is 1.5 to 2 times higher than the base alloy which consists of Fe, Ni, and Cr. This is also supported by the XRD result which shows that the rate of diffusion of elemental Fe, Cr and Ni is more when we add Y_2O_3 .

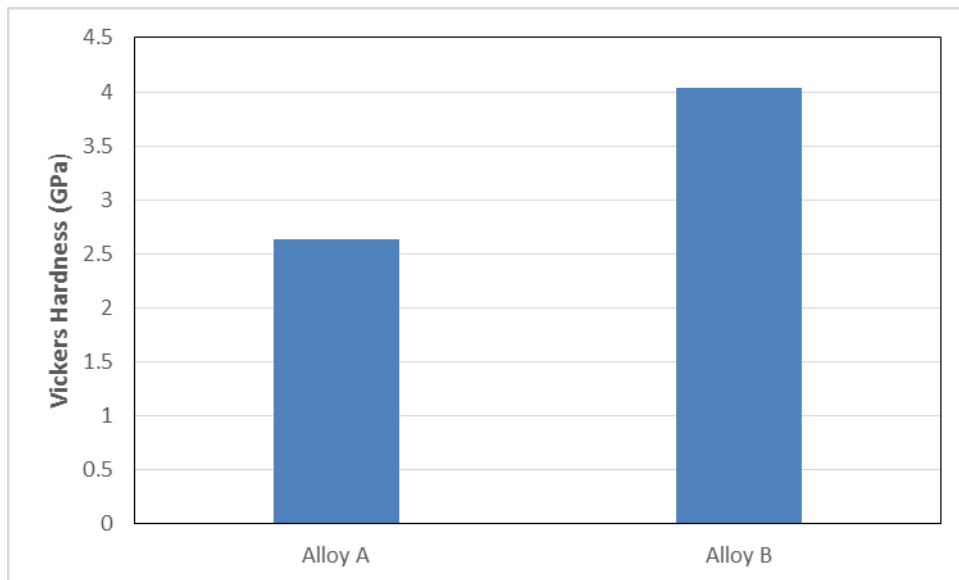


Fig 4.5: Hardness of sintered products (alloy A and alloy B)

4.5 DISCUSSION

The mechanical strength of the present alloys can be interpreted by various strengthening mechanisms such as dispersion hardening, solid solution hardening and grain refinement (Hall–Petch effect). Due to the sintering of these alloys at high temperature grain coarsening must have taken place and can't be neglected. So it is anticipated that strengthening effect due to grain refinement even if present in the as milled condition can't be considered after sintering. So strengthening due to dispersion and solid solution effects would dominate over grain refinement effect.

Dispersion strengthening in the current Y_2O_3 reinforced alloy is primarily based on the weight fraction, particle size and inter-particle spacing of fine Y_2O_3 in the matrix. The size and distribution of these fine phases are determined by nucleation, growth and coarsening rates during sintering.

5.0 Conclusion

The present study suggests that the detailed synthesis, microstructural characterization and mechanical property evaluation of the present nanocrystalline austenitic stainless steel (SS 304-L) as well as nano- Y_2O_3 dispersed austenitic nanocrystalline matrix by mechanical alloying and followed by conventional sintering at 1150°C for 1 h. The important conclusions that can be drawn from the results presented here are as following:

- ❖ It is possible to synthesize austenitic stainless steel (Fe-70%, Cr-19%, Ni-11%) powder from 0 to 40 h of milling by using planetary ball mill.
- ❖ After 30 h of milling, it is found that Cr and Ni completely dissolved in Fe matrix which was confirmed by XRD analysis.
- ❖ The particle size of the powder gets reduced as the milling proceeds, the size of the particle reduces from 63.6 μ m to 5.49 μ m during the milling of 40 hours by SEM analysis.

- ❖ It is found that the particle size of alloy powder synthesized goes to the nanometric range as observed during XRD and SEM studies.
- ❖ The current alloy follows solid solution strengthening, precipitation hardening and grain refinement.
- ❖ There is a 1.5-2 times improvement in hardness of alloy with 1.0 wt.% Y_2O_3 dispersed alloy than that of the base alloy

References:

- [1] C. Suryanarayana (Ed.), Oxford, 1999.
- [2] B.S Murty, S Ranganathan, Int. Mater. Rev., 43 (1998), pp. 101–141
- [3] M.O. Lai, L. Lu, Boston, MA, 1998.
- [4] C. Suryanarayana, Prog. Mater.Sci. 46 (2000) (in press).
- [5] Turker M, Karatas C, Saritas S, 12–16 November 2000, Kyoto, Japan, p. 1745–4
- [6] Kilinc Y, Turker M, Saritas S, 12–16 November 2000, Kyoto, Japan, p. 1701–04.
- [7] H. Arik, Mater Design, 25 (2004), pp. 31–40
- [8] C. Suryanarayana, Prog Mater Sci, 46 (2001), pp. 1–184
- [9] B.S.Murty ,S.Ranganathan, Rev 1998, Vol.43, pp.101-141.
- [10] K Upadhyya, PA, TMS, Warrendale, 1993.
- [11] RL Bickerdike, D Clark , JN Easterbrook, G Hughes, WN Mair , PG Partridge, HS Ranson:
“Internat J Rapid Solidification”, 1984, Vol.1, pp.305-330.
- [12] D.Turnbull: “Metall Trans”, 1981, Vol.12A, pp.695-708.
- [13] G Martin , P Bellon , 1997, Vol.50, pp.189-331.
- [14] K Okada , S Kikuchi , T Ban, N J Otsuka: “Mater SciLett”, 1992, Vol.11.
- [15] G Nicoara, D Fratiloiu, M Nogues, J L Dormann, F Vasiliu: “ MaterSci Forum”,1997.
- [16] Bellosi A, Montverde F, Botti S, Martelli S. Mater Sci Forum 1997, pp.235-238.
- [17] B P Dolgin , M A Vanek, T McGory , D J Ham: “ Non-Cryst Solids”, 1986, Vol.9, pp.87-281.
- [18] I Kerr: Rep 1993, Vol.48, pp.36-44.